# TROSY Triple-Resonance Four-Dimensional NMR Spectroscopy of a 46 ns Tumbling Protein

**Daiwen Yang* and Lewis E. Kay***

*Contribution from the Protein Engineering Network Centers of Excellence and the Departments of Medical and Molecular Genetics, Biochemistry and Chemistry, The University of Toronto, Toronto, Ontario, Canada, M5S 1A8*

*Received November 23, 1998. Revised Manuscript Received January 27, 1999*

**Abstract:** Two four-dimensional TROSY triple resonance based experiments are presented for backbone assignment of high molecular weight proteins and protein complexes. The experiments, 4D-HNCACO and 4D-HNCOCA, establish correlations of the form ($^{13}C^{\alpha}_{(i,i-1)}$,$^{13}C'_{(i,i-1)}$,$^{15}N_{(i)}$,$HN_{(i)}$) and ($^{13}C^{\alpha}_{(i-1)}$,$^{13}C'_{(i-1)}$,$^{15}N_{(i)}$,$HN_{(i)}$), respectively. Both sequences use an implementation of TROSY that offers improved sensitivity relative to previous sequences, critical for application to systems with correlation times on the order of 40−50 ns. The utility of the experiments is demonstrated by an application to a 46 ns tumbling complex of the 370 residue maltose binding protein and $\beta$-cyclodextrin. Approximately 95% of the expected intra- and interresidue correlations are observed in the HNCACO and HNCOCA, respectively, with average signal-to-noise values of approximately 35/1. The methodology promises to be particularly powerful for applications to high molecular weight complexes comprised of a labeled fragment and unlabeled components or proteins with segmental labeling.

## Introduction

The use of deuteration in concert with $^{15}N$, $^{13}C$ labeling of proteins has greatly extended the size limitations that are imposed on NMR studies of fully protonated molecules.[1] Assignment of backbone chemical shifts of proteins with correlation times on the order of 15−20 ns is now possible in many cases,[2−4] and solution structures of proteins and protein complexes in the 30 kDa molecular weight regime have been published.[5,6] Recently, Pervushin and co-workers have described a class of experiments which exploit the relaxation interference between $^{1}H-^{15}N$ dipolar and $^{15}N$ chemical shift anisotropy interactions that offer significant improvements in resolution and sensitivity in $^{1}H-^{15}N$ correlation experiments.[7] When combined with $^{2}H$-based triple-resonance schemes, these so-called TROSY experiments promise to increase the range of molecules amenable to study by NMR still further.[8,9]

Assignment of backbone NMR resonances of $^{15}N$, $^{13}C$-labeled proteins is based on a strategy in which chemical shifts from one residue are linked to those of sequential residues using a series of experiments which correlate $^{1}H$, $^{15}N$, and $^{13}C$ chemical shifts.[10] In the case of highly deuterated proteins, a family of HNC-type experiments has been developed which exploit the increased relaxation times of carbon spins bound to deuterons.[2,3,11−15] Frequently, $^{13}C$ chemical shifts are recorded in constant-time mode for a period of $1/J_{CC}$, where $J_{CC}$ is the one-bond $^{13}C-^{13}C$ aliphatic coupling constant.[16,17] The high resolution available in such spectra is absolutely critical in the case of large proteins, where resonance overlap can be severely limiting. In our laboratory these experiments have been successfully applied to the assignment of $^{13}C^{\alpha}$, $^{13}C^{\beta}$, $^{15}N$, and HN shifts of two protein systems that tumble in solution with correlation times of approximately 20 ns, including a 64 kDa complex of Trp-repressor and target DNA[3] and the 370 residue maltose binding protein (MBP) in complex with a heptasaccharide, $\beta$-cyclodextrin.[18] Studies of significantly higher molecular weight molecules, however, are likely to be hampered by lack of sensitivity and resolution. With this in mind we have developed a pair of TROSY-based 4D triple-resonance experiments which can be used for the study of larger proteins and protein complexes. An application to an $^{15}N$, $^{13}C$, $^{2}H$, [Leu, Val, Ile ($\delta$1 only)]-methyl-protonated sample of MBP/$\beta$-cyclodextrin at 5 °C with a correlation time of 46 ± 2 ns establishes the utility of the approach for high molecular weight systems.

(1) Gardner, K. H.; Kay, L. E. *Annu. Rev. Biophys. Biomol. Struct.* **1998**, *27*, 357−406.
(2) Yamazaki, T.; Lee, W.; Arrowsmith, C. H.; Muhandiram, D. R.; Kay, L. E. *J. Am. Chem. Soc.* **1994**, *116*, 11655−11666.
(3) Shan, X.; Gardner, K. H.; Muhandiram, D. R.; Rao, N. S.; Arrowsmith, C. H.; Kay, L. E. *J. Am. Chem. Soc.* **1996**, *118*, 6570−6579.
(4) Venters, R. A.; Farmer, B. T.; Fierke, C. A.; Spicer, L. D. *J. Mol. Biol.* **1996**, *264*, 1101−1116.
(5) Yu, L.; Petros, A. M.; Schnuchel, A.; Zhong, P.; Severin, J. M.; Walter, K.; Holzman, T. F.; Fesik, S. W. *Nat. Struct. Biol.* **1997**, *4*, 483−489.
(6) Garrett, D. S.; Seok, Y. J.; Liao, D. I.; Peterkofsky, A.; Gronenborn, A. M.; Clore, G. M. *Biochemistry* **1997**, *36*, 2517−2530.
(7) Pervushin, K.; Riek, R.; Wider, G.; Wüthrich, K. *Proc. Natl. Acad. Sci. U.S.A.* **1997**, *94*, 12366−12371.
(8) Yang, D.; Kay, L. E. *J. Biomol. NMR* **1999**, *13*, 3−9.
(9) Salzmann, M.; Pervushin, K.; Wider, G.; Senn, H.; Wüthrich, K. *Proc. Natl. Acad. Sci. U.S.A.* **1998**, *95*, 13585−13590.
(10) Bax, A. *Curr. Opin. Struct. Biol.* **1994**, *4*, 738−744.
(11) Grzesiek, S.; Anglister, J.; Ren, H.; Bax, A. *J. Am. Chem. Soc* **1993**, *115*, 4369−4370.
(12) Yamazaki, T.; Lee, W.; Revington, M.; Mattiello, D. L.; Dahlquist, F. W.; Arrowsmith, C. H.; Kay, L. E. *J. Am. Chem. Soc.* **1994**, *116*, 6464−6465.
(13) Farmer, B. T.; Venters, R. *J. Am. Chem. Soc.* **1995**, *117*, 4187−4188.
(14) Farmer, B. T.; Venters, R. A. *J. Biomol. NMR* **1996**, *7*, 59−71.
(15) Dötsch, V.; Matsuo, H.; Wagner, G. *J. Magn. Reson. Ser. B* **1996**, *112*, 95−100.
(16) Vuister, G. W.; Bax, A. *J. Magn. Reson.* **1992**, *98*, 428−435.
(17) Santoro, J.; King, G. C. *J. Magn. Reson.* **1992**, *97*, 202−207.
(18) Gardner, K. H.; Zhang, X.; Gehring, K.; Kay, L. E. *J. Am. Chem. Soc.* **1998**, *120*, 11738−11748.

10.1021/ja984056t CCC: $18.00 © 1999 American Chemical Society
Published on Web 03/06/1999

## Materials and Methods

All spectra were recorded on a 1.4 mM sample of $^{15}N$, $^{13}C$, $^{2}H$, [Leu, Val, Ile ($\delta$1 only)]-methyl-protonated MBP/$\beta$-cyclodextrin, 20 mM sodium phosphate buffer (pH 7.2), 3 mM $NaN_3$, 100 mM EDTA, 0.1 mg/mL Pefabloc, 1 $\mu$g/$\mu$L pepstatin, 10% $D_2O$, prepared as described previously.[18] Experiments were recorded on a Varian Inova 600 MHz spectrometer. A separate rf channel was used for each of the $^{1}H$, $^{15}N$, $^{13}C$, and $^{2}H$ pulses. The $^{2}H$ lock receiver was disabled during application of either $^{2}H$ pulses/decoupling or pulsed field gradients. The HNCACO data set was acquired as a complex matrix consisting of (23,14,36,576) complex data points, corresponding to acquisition times of (8.15 ms, 8.6 ms, 21.9 ms, 64 ms) in the ($^{13}C^{\alpha}$,$^{13}C'$,$^{15}N$,HN) dimensions. A relaxation delay of 1.4 s was employed along with 4 scans/FID, giving rise to a net acquisition time of 7 days. Data processing was performed with NMRPipe/NMRDraw[19] software and spectra analyzed with NMRView.[20] Briefly, mirror image linear prediction[21] was employed to double the $^{13}C^{\alpha}$ and $^{15}N$ time domains, with forward−backward linear prediction[22] used to double the $^{13}C'$ dimension. Linear prediction in a given dimension was performed only after all three other dimensions were transformed, as described by Kay et al.[23] Cosine-bell window functions were employed in each of $t_1$ and $t_3$, a cosine-squared window was used in $t_2$, and the $t_4$ dimension was apodized with a sinebell-squared window shifted by 80°. After linear prediction and zero-filling, the final data set, which included only the region where correlations were present, was comprised of (128,64,128,256) real points. The HNCOCA data set consisted of (14,21,34,576) complex data points, with acquisition times of (8.6 ms, 7.4 ms, 20.6 ms, 64 ms) in the ($^{13}C'$,$^{13}C^{\alpha}$,$^{15}N$,HN) dimensions and a total experimental time of 6 days (1.4 s repetition delay, 4 scans/FID). Mirror image linear prediction was employed to double the $^{13}C'$ and $^{15}N$ time domains while the $^{13}C^{\alpha}$ dimension was extended 2-fold by forward−backward linear prediction. The window functions employed were as described for the HNCACO. The final data set consisted of (64,128,128,256) real points. The NMRPipe scripts used for processing and the pulse sequence codes are available on request.

## Results and Discussion

Figure 1 illustrates the two 4D triple-resonance experiments that we have applied with success to the study of MBP at 5 °C. The pulse sequences are derived from 3D HN(CO)CA and HN(CA)CO schemes that have been described in the literature previously,[24,25] and only a brief summary of the sequences will be provided here. The magnetization transfer steps in each of the experiments can be summarized by the following pathways for the 4D HNCOCA and HNCACO, respectively,

$$\mathrm{HN}_{(i)} \xrightarrow{J_{HN}} {}^{15}\mathrm{N}_{(i)} \xrightarrow{J_{NC'}} {}^{13}\mathrm{C}'_{(i-1)}\,[t_1] \xrightarrow{J_{C'C\alpha}} {}^{13}\mathrm{C}^{\alpha}_{(i-1)}\,[t_2] \xrightarrow{J_{C'C\alpha}} {}^{13}\mathrm{C}'_{(i-1)} \xrightarrow{J_{NC'}} {}^{15}\mathrm{N}_{(i)}\,[t_3] \xrightarrow{J_{HN}} \mathrm{HN}_{(i)}\,[t_4]$$

$$\mathrm{HN}_{(i)} \xrightarrow{J_{HN}} {}^{15}\mathrm{N}_{(i)} \xrightarrow{J_{NC\alpha}} {}^{13}\mathrm{C}^{\alpha}_{(i-1,i)}\,[t_1] \xrightarrow{J_{C'C\alpha}} {}^{13}\mathrm{C}'_{(i-1,i)}\,[t_2] \xrightarrow{J_{C'C\alpha}} {}^{13}\mathrm{C}^{\alpha}_{(i-1,i)} \xrightarrow{J_{NC\alpha}} {}^{15}\mathrm{N}_{(i)}\,[t_3] \xrightarrow{J_{HN}} \mathrm{HN}_{(i)}\,[t_4] \quad (1)$$

Of particular importance is that the TROSY principle[7] is employed in both $^{15}N$ and HN dimensions. In this approach, only one of the two possible $^{15}N$ components, corresponding to slowly relaxing $^{15}N$ transverse magnetization coupled to the $\beta$ proton spin state, is preserved. By ensuring that $^{15}N$ components associated with $\alpha$ and $\beta$ states are not interchanged during the pulse sequence and that the signal from the slowly relaxing $^{15}N$ component is transferred to the slowly relaxing proton multiplet component for detection, significant sensitivity gains can be achieved.[7,26,27] As described in detail previously,[8] we prefer to implement TROSY using a pulse scheme that is somewhat different from the sequence proposed by Pervushin, Wüthrich, and co-workers.[9,27] In the case of the methodology presented by this group, selection of the slowly relaxing multiplet component is achieved by using either a phase cycling or gradient procedure. Of the two possible pathways, denoted by $N_{TR}(1 \pm 2HN_Z) \rightarrow HN_{TR}(1 \mp 2N_Z)$, where $X_{TR}$ and $X_Z$ correspond to transverse and longitudinal X magnetization, respectively, only the $N_{TR}(1 - 2HN_Z) \rightarrow HN_{TR}(1 + 2N_Z)$ path is retained. This transfer of magnetization from $^{15}N$ to HN prior to detection proceeds via the establishment of transverse and double/zero quantum spin states that relax efficiently in large molecules. In contrast, the scheme that we employ relies on a slightly modified version of the enhanced sensitivity[28] pulsed field gradient sequence developed previously.[29,30] In this approach both pathways $N_{TR}(1 \pm 2HN_Z) \rightarrow HN_{TR}(1 \mp 2N_Z)$ are preserved. For triple resonance applications involving large molecules at high fields, the undesired pathway [$N_{TR}(1 + 2HN_Z) \rightarrow HN_{TR}(1 - 2N_Z)$ ] is effectively suppressed by relaxation during the pulse scheme, as described previously.[8] Thus in both implementations cross-peaks are observed at $^{15}N$,HN coordinates of $\omega_N - \pi J_{NH}$, $\omega_H + \pi J_{NH}$, $J_{NH} < 0$. However, because signal resides along the *Z*-axis for significant periods during the $^{15}N \rightarrow$ HN transfer in the case of the enhanced sensitivity pulsed field gradient scheme, relaxation losses are minimized.[8] In the case of MBP at 5 °C, where a correlation time of 46 ± 2 ns is measured by $^{15}N$ spin relaxation,[31] an average sensitivity gain of 20% is noted in TROSY-based HNC triple-resonance spectra using this scheme relative to methodology described by Pervushin et al.[27]

A second point of interest concerns the 4D HNCOCA sequence. Unlike the 3D CT-HN(CO)CA experiment that we published previously,[2] the $^{13}C^{\alpha}$ chemical shift is not recorded in constant-time (CT) mode in the 4D experiment. The use of a constant-time $^{13}C^{\alpha}$ acquisition period of $\approx 1/J_{CC}$ that we employed in the case of the 3D experiment becomes particularly costly in terms of sensitivity in the case of applications to proteins with correlation times on the order of 40−50 ns. For example, $^{13}C^{\alpha}$ free precession $T_2$ values (recorded with $^{2}H$ decoupling) averaging 38 ± 10 ms have been measured via a modified HN(COCA) sequence for 29 well-resolved residues in the $^{1}H-^{15}N$ spectrum of deuterated MBP at 25 °C (correlation time, $\tau_C$, of 23 ± 0.8 ns). It is noteworthy that this value is significantly lower than the average $^{13}C^{\alpha}$ $T_{1\rho}$ value, 85 ± 20 ms, measured for the same residues. The origin of this discrepancy is not understood at the moment, although it is interesting that substantial differences in $^{13}C^{\alpha}$ $T_2$ and $T_{1\rho}$ values

(19) Delaglio, F.; Grzesiek, S.; Vuister, G. W.; Zhu, G.; Pfeifer, J.; Bax, A. *J. Biomol. NMR* **1995**, *6*, 277−293.
(20) Johnson, B. A.; Blevins, R. A. *J. Biomol. NMR* **1994**, *4*, 603−614.
(21) Zhu, G.; Bax, A. *J. Magn. Reson.* **1990**, *90*, 405−410.
(22) Zhu, G.; Bax, A. *J. Magn. Reson.* **1992**, *98*, 192−199.
(23) Kay, L. E.; Ikura, M.; Zhu, G.; Bax, A. *J. Magn. Reson.* **1991**, *91*, 422−428.
(24) Bax, A.; Ikura, M. *J. Biomol. NMR* **1991**, *1*, 99−104.
(25) Clubb, R. T.; Thanabal, V.; Wagner, G. *J. Magn. Reson.* **1992**, *97*, 213-217.
(26) Pervushin, K.; Riek, R.; Wider, G.; Wüthrich, K. *J. Am. Chem. Soc.* **1998**, *120*, 6394−6400.
(27) Pervushin, K. V.; Wider, G.; Wüthrich, K. *J. Biomol. NMR* **1998**, *12*, 345−348.
(28) Palmer, A. G.; Cavanagh, J.; Wright, P. E.; Rance, M. *J. Magn. Reson.* **1991**, *93*, 151−170.
(29) Kay, L. E.; Keifer, P.; Saarinen, T. *J. Am. Chem. Soc.* **1992**, *114*, 10663−10665.
(30) Schleucher, J.; Sattler, M.; Griesinger, C. *Angew. Chem., Int. Ed. Engl.* **1993**, *32*, 1489−1491.
(31) Farrow, N. A.; Muhandiram, R.; Singer, A. U.; Pascal, S. M.; Kay, C. M.; Gish, G.; Shoelson, S. E.; Pawson, T.; Forman-Kay, J. D.; Kay, L. E. *Biochemistry* **1994**, *33*, 5984−6003.

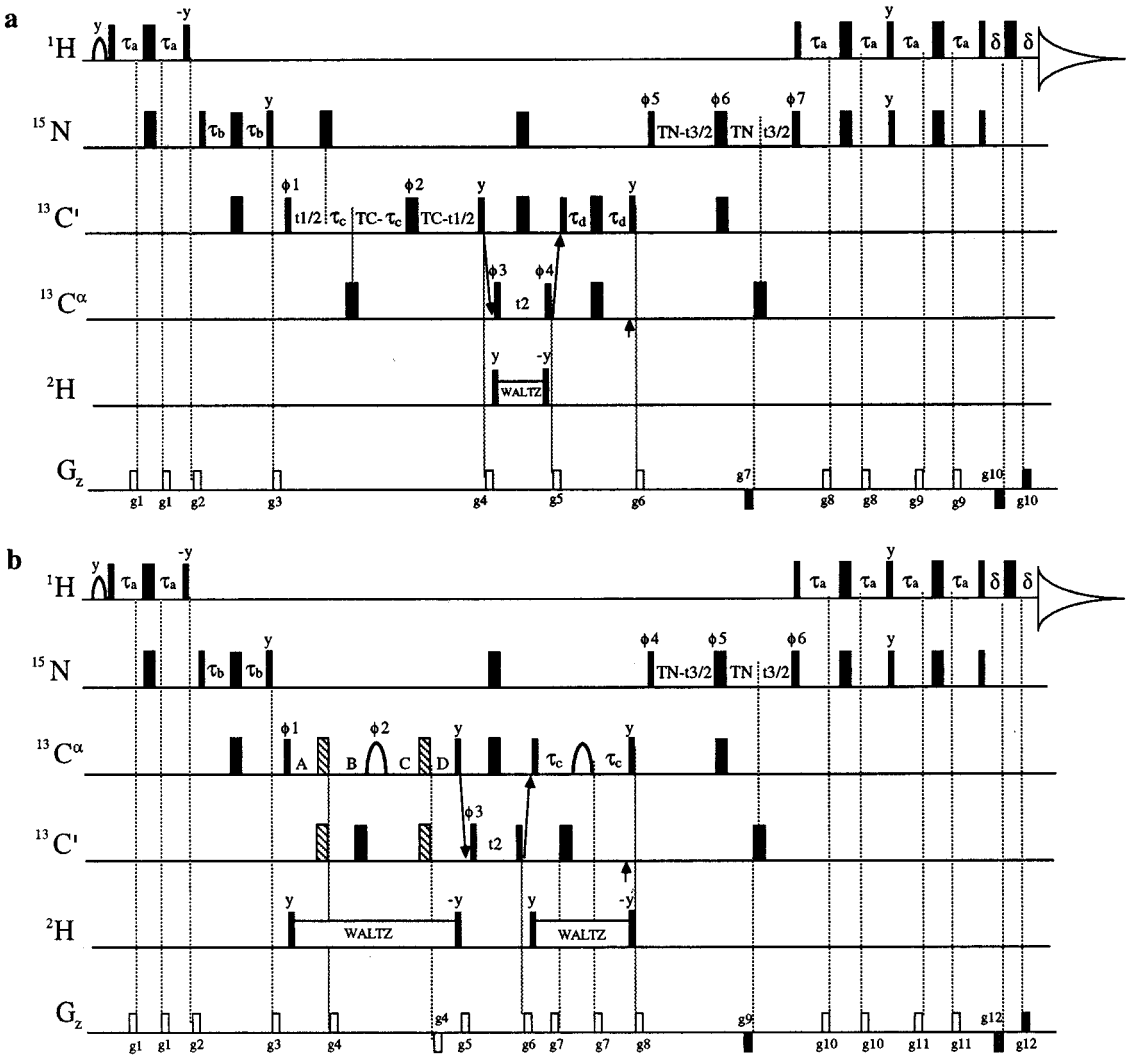


**Figure 1.** Pulse schemes of the HNCOCA (a) and HNCACO (b) experiments. All narrow (wide) pulses are applied with flip angles of 90° (180°) along the *x*-axis, unless indicated otherwise. The $^1$H and $^{15}$N carriers are positioned at 4.72 (water) and 119 ppm, respectively, and all proton pulses are applied with a field of 32 kHz (with the exception of the shaped 90° water selective pulse which has the EBURP-1 profile[32] (7.1 ms, 1.05 kHz)), while all $^{15}$N pulses employ a 6.2 kHz field. Note that depending on the spectrometer brand the phase of the second $^1$H 90° pulse may have to be changed from $-y$ to $y$ to ensure that magnetization arising from both the $^{15}$N and HN originating components adds constructively.[26,27] The phase listed is correct for Varian spectrometers. (a) The $^{13}$C carrier is set to 176 ppm, switched to 55 ppm immediately prior to the $^{13}$C$^\alpha$ pulse of phase $\phi 3$, and returned to 176 ppm after the following $^{13}$C$^\alpha$ pulse (phase $\phi 4$). All $^{13}$C′ and $^{13}$C$^\alpha$ 90° (180°) pulses are applied with a field strength of $\Delta/\sqrt{15}$ ($\Delta/\sqrt{3}$), where $\Delta$ is the separation in Hz between the centers of the $^{13}$C$^\alpha$ and $^{13}$C′ spectra.[35] Note that $^{13}$C′ 180° pulses in both sequences a and b can be applied as shaped pulses, having for example the seduce-1 profile.[36] The vertical arrow at the end of the second $\tau_d$ delay indicates the position of application of the $^{13}$C$^\alpha$ Bloch−Siegert compensation pulse[16] (note that the $^{13}$C$^\alpha$ pulse in the center of the $2\times\tau_d$ period is applied prior to the $^{13}$C′ pulse). The delays used are: $\tau_a = 2.2$ ms; $\tau_b = 12.0$ ms; $\tau_c = 4.25$ ms; $\tau_d = 4.0$ ms; TC = 4.3 ms, $\delta = 0.25$ ms; TN = 12.0 ms. The phase cycling employed is: $\phi 1 = x$; $\phi 2 =$ x, $y$, $-x$, $-y$; $\phi 3 = x$; $\phi 4 = 2(x)$, $2(-x)$; $\phi 5 = y$; $\phi 6 = 2(x)$, $2(-x)$; $\phi 7 = x$; rec = $x$, $2(-x)$, $x$. Quadrature detection in $F_1$ and $F_2$ is achieved by States-TPPI[37] of $\phi 1$ and $\phi 3$, respectively, while quadrature in $F_3$ employs the enhanced sensitivity pulsed field gradient method,[29,30] where for each value of $t_3$ separate data sets are recorded for (g7, $\phi 7$) and ($-$g7, $\phi 7+180°$). For each successive $t_3$ value $\phi 5$ and the phase of the receiver are incremented by 180°. The duration and strengths of the gradients are: g1 = (0.4 ms, 5 G/cm); g2 = (1 ms, 10 G/cm); g3 = (0.7 ms, 10 G/cm); g4 = (0.6 ms, −15 G/cm); g5 = (0.5 ms, 12 G/cm); g6 = (0.5 ms, 15 G/cm); g7 = (1.25 ms, −30 G/cm); g8 = (0.4 ms, 3.1 G/cm); g9 = (0.4 ms, 5.35 G/cm); g10 = (62.5 $\mu$s, 28.75 G/cm). (b). The $^{13}$C carrier is set to 55 ppm, jumped to 176 ppm prior to the $^{13}$C′ 90° pulse of phase $\phi 3$, and returned to 55 ppm after the subsequent $^{13}$C′ 90° pulse. All $^{13}$C′ and $^{13}$C$^\alpha$ 90° pulses are applied with a field strength of $\Delta/\sqrt{15}$ while the filled rectangular 180° pulses use a field of $\Delta/\sqrt{3}$. The shaped $^{13}$C$^\alpha$ refocusing pulses have the REBURP profile[32] and are of duration (1000/$y$) ms, where $y$ is the spectrometer field (in MHz). For the present application at 600 MHz, 1.6 ms pulses were employed (3.8 kHz peak rf). The "shaded" pulses (indicated as simultaneous $^{13}$C$^\alpha$/$^{13}$C′ pulses in the diagram) were applied as single composite (nonselective) 180° pulses ($90_x180_y90_x$) centered at 55 ppm with a field strength of 20.8 kHz (600 MHz). Simulations using the Bloch equations establish that a composite 180° pulse of field strength 20.8 kHz × ($y$/600), where $y$ is the spectrometer frequency in MHz, refocuses over the $^{13}$C$^\alpha$ bandwidth and inverts the $^{13}$C′ spins (≥97%). Current generation 800 MHz spectrometer probes can deliver pulses at the ≈28 kHz field strength necessary for the proper inversion of $^{13}$C′ spins; in cases where the field strength is insufficient the shaded pulses can be replaced by high-power (nonselective for aliphatic) REBURP[32] (350 $\mu$s 180°, 17.8 kHz) and selective $^{13}$C′ pulse pairs. The vertical arrow indicates the position of the $^{13}$C′ Bloch−Siegert compensation pulse.[16] The delays used are: $\tau_a = 2.2$ ms; $\tau_b = 12$ ms; $\tau_c = 4$ ms; TN = 12 ms; $\delta = 0.25$ ms; $A = (T_C - t_1)/4$; $B = (T_C + t_1)/4$; $C = (T_C - t_1)/4$; $D = (T_C + t_1)/4$; $T_C = 8.2$ ms. The phase cycling employed is: $\phi 1 = x$; $\phi 2 = x, y, -x, -y$; $\phi 3 = 2(x)$, $2(-x)$; $\phi 4 = y$; $\phi 5 = 2(x)$, $2(-x)$; $\phi 6 = x$; rec = $x$, $2(-x)$, $x$. Quadrature detection in $F_1$ and $F_2$ are achieved by States-TPPI[37] of $\phi 1$ and $\phi 3$, respectively, while for each value of $t_3$ separate data sets are recorded for (g9, $\phi 6$) and ($-$g9, $\phi 6 + 180°$). For each successive $t_3$ value $\phi 4$ and the phase of the receiver are incremented by 180°. The duration and strengths of the gradients are: g1 = (0.4 ms, 5 G/cm); g2 = (0.8 ms, 15 G/cm); g3 = (0.9 ms, 10 G/cm); g4 = (0.1 ms, 15 G/cm); g5 = (0.6 ms, −15 G/cm); g6 = (0.5 ms, 12 G/cm); g7 = (80 $\mu$s, 20 G/cm); g8 = (0.4 ms, 15 G/cm); g9 = (1.25 ms, −30 G/cm); g10 = (0.4 ms, 3.1 G/cm); g11 = (0.4 ms, 5.35 G/cm); g12 = (62.5 $\mu$s, 28.75 G/cm). Decoupling is interrupted prior to the application of the gradients.[38]

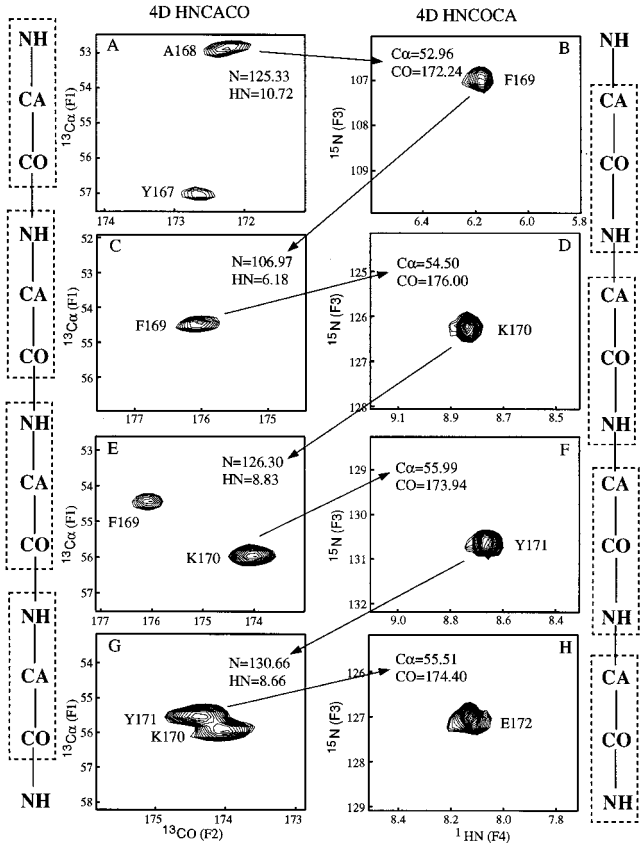


**Figure 2.** Representative $^{13}C^{\alpha}-^{13}C'$ and $^{15}N-^{1}HN$ planes from the 4D HNCACO and 4D HNCOCA data sets of a 1.4 mM $^{15}N$, $^{13}C$, $^{2}H$, [Leu, Val, Ile ($\delta$1 only)]-methyl-protonated MBP/$\beta$-cyclodextrin complex at 5 °C ($\tau_C = 46 \pm 2$ ns) illustrating the assignment strategy used. Two of the four chemical shifts associated with each peak are indicated on each plane. Note that in the HNCACO both inter- and intraresidue correlations can be observed. Cross-peaks are labeled on the basis of the $^{13}C^{\alpha}$,$^{13}C'$ or $^{15}N$, HN chemical shifts in 4D HNCACO and 4D HNCOCA spectra, respectively.

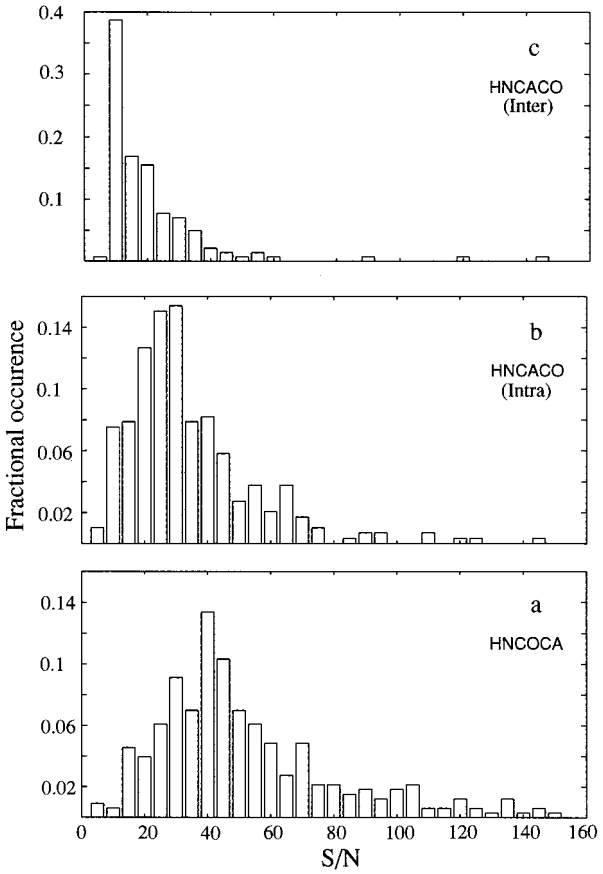


**Figure 3.** Distributions of peak signal-to-noise (S/N) ratios for the 4D HNCOCA (a) and 4D HNCACO (b, intraresidue; c, interresidue) experiments recorded on MBP at 5 °C (600 MHz).

have also been measured for fully protonated ubiquitin. Assuming that the free precession $T_2$ values will scale roughly inversely with $\tau_C$ and noting that the sensitivity ratio of the non-CT to the CT experiment is given to excellent approximation as,

$$R = 1/(\mathrm{AT}) \int_{\mathrm{AT}} \cos(\pi J_{CC} t) \exp(-t/T_2)\, \mathrm{d}t_2/\exp(-T/T_2) \quad (2)$$

where AT is the total acquisition time in the $^{13}C^{\alpha}$ dimension in the non-CT experiment (7.4 ms in the case of the 4D HNCOCA), $T$ is the duration of the CT period (typically $\approx$ 28 ms), and $T_2$ is the free precession transverse $^{13}C^{\alpha}$ relaxation time (in the presence of $^{2}H$ decoupling), $R \approx 3$ for MBP at 5 °C. Such a decrease in sensitivity is considerable especially in lieu of losses during other delays in the pulse scheme. For example, on doubling the correlation time from 23 to 46 ns, results on MBP at 600 MHz indicate a decrease of a factor of at least 4 in the intensity of correlations obtained in the TROSY-HNCO[8] (quantitated as peak heights), and calculations suggest a similar loss at 800 MHz. Experiments that involve more complex magnetization transfer schemes will experience additional loses. The 4D experiments that are proposed here offer both improved sensitivity and resolution relative to their CT 3D counterparts for applications to very large molecular complexes (correlation times on the order of 40−50 ns).

A final point of note concerns the HNCACO experiment. During the transfer of magnetization from $^{13}C^{\alpha}$ to $^{13}C'$ (and back) evolution due to passive $^{13}C^{\alpha}-^{13}C^{\beta}$ couplings attenuates the signal. We have employed a scheme in which selective $^{13}C^{\alpha}$ pulses are applied at the center of the transfer periods, resulting in refocusing of evolution due to $J_{C\alpha C\beta}$. These selective pulses have the REBURP profile,[32] are centered at 55 ppm, and have a duration of (1000/$y$) ms, where $y$ is the spectrometer field strength in MHz. For the majority of residues, the $^{13}C^{\alpha}-^{13}C^{\beta}$ couplings are refocused with this approach and sensitivity losses are therefore minimized. A number of residues, however, such as Gly, Val, and Pro may have $^{13}C^{\alpha}$ shifts outside the window of refocusing (63.3 to 46.7 ppm), while the $^{13}C^{\beta}$ spins of many Ser residues may be affected by the pulse. Sensitivity losses for these residue are likely, and we have therefore recorded a 3D HNCA experiment (non-CT) to supplement correlations from the HNCACO data set. It is noteworthy that alternative schemes such as $^{13}C^{\beta}$ decoupling with adiabatic pulse trains may also be employed to minimize evolution due to $^{13}C^{\alpha}-^{13}C^{\beta}$ couplings,[33] but we have not attempted this here.

Figure 2 illustrates the quality of the data obtained for a 1.4 mM sample of $^{15}N$, $^{13}C$, $^{2}H$, [Leu, Val, Ile ($\delta$1 only)]-methyl-protonated MBP/$\beta$-cyclodextrin at 5 °C, 600 MHz. Analysis of the two 4D data sets is straightforward, as illustrated in the figure. Starting from slice A, the $^{13}C^{\alpha}$, $^{13}C'$ coordinates of the peak denoted by Ala168 in the HNCACO are used to obtain the $^{15}N$,$^{1}HN$ coordinates of the successive residue from the HNCOCA. The $^{15}N$,$^{1}HN$ shifts of Phe169 are subsequently used to measure the intraresidue $^{13}C^{\alpha}$,$^{13}C'$ shifts from the HNCACO, and the process is continued for the succeeding residues. The

(32) Geen, H.; Freeman, R. *J. Magn. Reson.* **1991**, *93*, 93−141.
(33) Matsuo, H.; Kupce, E.; Li, H.; Wagner, G. *J. Magn. Reson.* **1996**, *113*, 91−96.

approach is illustrated for residues Ala168−Glu172. Difficulty in assignment arises if two or more residues in the protein have degenerate ($^{15}$N,$^{1}$HN) or ($^{13}C^{\alpha}$,$^{13}C'$) spin pairs. In these cases all potential assignments must be retained until some point in the assignment process where it becomes possible to distinguish between the choices. Unfortunately, this is difficult to do with the present set of experiments since only a few residues have distinctive $^{13}C^{\alpha}$ chemical shifts. Therefore, additional information will very likely be required to obtain compete assignments of large proteins. However, the fact that over 93% and 96% of the expected intraresidue HNCACO and interresidue HNCOCA correlations were observed in the present study, respectively (44% of the expected interresidue peaks from the HNCACO were noted as well), suggests that it may be possible to assign large complexes where one component of less than approximately 200 residues is labeled while the other component(s) is (are) not. This is especially the case if assignments of the labeled molecule in the uncomplexed state are also available. For example, starting from the assignments available for MBP at 37 °C,[18] we were able to obtain assignments at a similar completeness level for the molecule at 5 °C using the two 4D experiments described above as well as a non-CT HNCA.

Figure 3 shows histograms of the percent occurrence of cross-peaks vs signal-to-noise (S/N) for the 4D HNCOCA (a) and intra- (b) and interresidue (c) correlations observed in the 4D HNCACO. The S/N is really quite remarkable for a protein tumbling with a correlation time of 46 ns.

In summary, we have described two 4D TROSY-based triple-resonance experiments for protein backbone assignment. The TROSY scheme has been implemented by using the enhanced sensitivity pulsed field gradient approach[8] which, for applications involving molecules with large correlations times, results in substantial sensitivity improvements. The high sensitivity of the data obtained for MBP at 5 °C suggests that these experiments will be particularly valuable for studying a labeled component as part of a high molecular weight complex or for investigating a defined region of a large protein by using the intein labeling strategy recently proposed by Yamazaki and co-workers.[34]

**Acknowledgment.** Dedicated to Professor Ray Freeman in appreciation of his many contributions to NMR spectroscopy. This research was supported by a grant from the Medical Research Council of Canada (L.E.K.). The authors thank Dr. K. Gardner and Mr. Randy Willis for preparation of the MBP sample. L.E.K. is a foreign investigator of the Howard Hughes Medical Research Institute.

**Supporting Information Available:** TROSY-based triple resonance 3D CT-HNCA, CT-HN(CO)CA, CT-HN(COCA)-CB, and CT-HN(CA)CB pulse schemes[2,3,12] using a variant of the enhanced sensitivity pulsed field gradient method for $^{15}$N−HN transfer prior to acquisition[8] as well as pulse sequences with active suppression of the undesired component in cases where relaxation does not suffice which are based on the pulsed gradient methods described here and in ref 8 (PDF). This material is available free of charge via the Internet at http://pubs.acs.org.

JA984056T

(34) Yamazaki, T.; Otomo, T.; Oda, N.; Kyogoku, Y.; Uegaki, K.; Ito, K.; Ishino, Y.; Nakamura, H. *J. Am. Chem. Soc.* **1998**, *120*, 5591−5592.
(35) Kay, L. E.; Ikura, M.; Tschudin, R.; Bax, A. *J. Magn. Reson.* **1990**, *89*, 496−514.
(36) McCoy, M.; Mueller, L. *J. Am. Chem. Soc.* **1992**, *114*, 2108−2110.
(37) Marion, D.; Ikura, M.; Tschudin, R.; Bax, A. *J. Magn. Reson.* **1989**, *85*, 393−399.
(38) Kay, L. E. *J. Am. Chem. Soc.* **1993**, *115*, 2055−2056.